

**NJC**

Cooperative halogen bonding and polarized π -stacking in the formation of coloured charge-transfer co-crystals

Journal:	<i>New Journal of Chemistry</i>
Manuscript ID	NJ-ART-02-2018-000693.R1
Article Type:	Paper
Date Submitted by the Author:	17-Mar-2018
Complete List of Authors:	Nwachukwu, Chideraa; Missouri State University, Chemistry Kehoe, Zachary; University of Wisconsin-Stevens Point, Chemistry Bowling, Nathan; University of Wisconsin-Stevens Point, Chemistry Speetzen, Erin; UW-Stevens Point, Chemistry Bosch, Eric; Missouri State University, Chemistry

SCHOLARONE™
Manuscripts



Journal Name

ARTICLE

Received 00th January 20xx,
Accepted 00th January 20xx

DOI: 10.1039/x0xx00000x

www.rsc.org/

Cooperative halogen bonding and polarized π -stacking in the formation of coloured charge-transfer co-crystals

Chideraa I. Nwachukwu,^a Zachary R. Kehoe,^b Nathan P. Bowling,^b Erin D. Speetzen^b and Eric Bosch^{a*}

Red co-crystals are formed between the matched complementary electron rich halogen bond acceptors, isomeric 4-(N,N-dimethylamino)phenylethynylpyridines and the electron poor halogen bond donor, 1-(3,5-dinitrophenylethynyl)-2,3,5,6-tetrafluoro-4-iodobenzene. The red 1:1 cocrystals exhibit strong halogen bonding and strong π -stacking. The N...I distances range from 2.80 to 2.85 Å and the C-I...N angles are between 169.9 and 175.8. In all four structures the donor and acceptor molecules are alternately π -stacked with the centroid to centroid distances between the dinitrophenyl moiety and the dimethylaminophenyl moiety between 3.61 and 3.73 Å. The calculated π - π stacking binding energy is -22.24 kcal/mol for the complex between 4-[4-(N,N-dimethylamino)phenylethynyl]pyridine and 1-(3,5-dinitrophenylethynyl)-2,3,5,6-tetrafluoro-4-iodobenzene while the calculated halogen bond binding energy between the same couple is -7.97 kcal/mol.

Introduction

The cooperative interplay between non-covalent interactions is ubiquitous and important in both solutions and crystalline solids that include neutral or charged organic moieties. Halogen bonding, an attractive non-covalent interaction that involves the attraction of a Lewis base to an electropositive region, has been employed as a controlling design feature across many disciplines including supramolecular chemistry, crystal engineering, molecular recognition, anion recognition, medicinal chemistry and synthetic organic and polymer chemistry.¹ The positioning of neighbouring electron withdrawing substituents enhances the electropositive region, the σ -hole, on the halogen bond donor leading to stronger interactions. Consequently, polyfluorohaloalkanes and arenes are widely used to direct cocrystallization through halogen bonding.¹ Nitro substituted iodobenzenes and charge assisted halogen bond donors have also been employed.^{2,3} The interplay between conventional hydrogen bonding and halogen bonding has been explored over the past several years.⁴ In this manuscript we will explore systems that probe cooperative halogen bonding and π - π complexation. Charge-transfer (CT) complexes, formed between an electron donor

^a Department of Chemistry, Missouri State University, 901 South National Avenue, Springfield, MO, 65897

^b Department of Chemistry, University of Wisconsin-Stevens Point, 2001 Fourth Avenue, Stevens Point, WI, 54481

† Footnotes relating to the title and/or authors should appear here.

Electronic Supplementary Information (ESI) available: [details of any supplementary information available should be included here]. See DOI: 10.1039/x0xx00000x

and an electron acceptor, have found application in a variety of areas notably molecular electronics and photonics. Segregated stacking of donor molecules and acceptor molecules (...-D-D... and ...-A-A-A...) is a necessity for metallic conductivity at room temperature while semiconductor properties are common with mixed stacks of alternating donor and acceptor molecules (...-D-A-D-A...).⁵ The formation of CT complexes as discrete entities along organic and organometallic reaction pathways has been demonstrated.⁶ A particularly elegant example of the application of the role of coloured π -stacked CT complexes in synthesis, was the CT complex directed synthesis of rotoxanes.⁷ While hexafluorobenzene forms colourless π -stacked cocrystals with a wide variety of arenes,⁸ *m*-dinitrobenzene forms coloured co-crystals with electron rich amino arenes.⁹ It is thus reasonable to incorporate cooperative halogen bonding and charge-transfer complexation into π -stacked cocrystals. In a study of the cocrystallization of bromo- and iododinitrobenzenes with tetramethyl-*p*-phenyl enediamine, π -stacking was observed with mixed stacks of donor and acceptor without halogen bonding.¹⁰ The π -stacking interaction was calculated to be 6-12 kcalmol⁻¹ more favourable than halogen bonding in these cocrystals. In a separate study of cocrystals formed between diaminonaphthalene and tetrahalo-1,4-benzoquinones, halogen bonding in the cocrystal formed with tetraiodobenzoquinone resulted in segregated stacks of donor and acceptor whereas the tetrabromo- and tetrachloroquinone cocrystals did not include halogen bonds and mixed stacks of donor and acceptor molecules were observed.¹¹ Our study was initiated after we observed that the yellow-orange co-crystal formed between 3,5-dinitro-1-iodobenzene and *N,N*-dimethylaminopyridine featured both strong halogen bonded and π -stacks of alternating donor and acceptor molecules. Herein we report the deliberate formation of cocrystals featuring halogen bonds and π -stacking.

Results and discussion

Preliminary results.

The asymmetric unit of the 1:1 cocrystal **A**, formed between 3,5-dinitro-1-iodobenzene and 4-(*N,N*-dimethylamino)pyridine, features a strong halogen bond with a N...I distance of 2.8937(1) Å, 82% of the sum of the van der Waals radii,¹² and C-I...N angle of 175.27°(6). Figure 1 shows the asymmetric unit of the halogen bonded cocrystal. The two nitro groups are coplanar with the benzene ring, with maximum distance of oxygen below the plane of the benzene ring of 0.154(3) Å, and the dimethylamino group is coplanar with the pyridine ring with the maximum distance of the methyl group above the plane of the pyridine ring of 0.134(4)Å.¹³ The dihedral angle between the two planes defined by the two aromatic compounds is 14.93(7)° and the packing features asymmetric

offset π -stacks of alternating 3,5-dinitro-1-iodobenzene and 4-(*N,N*-dimethylamino)pyridine molecules with two distinct π - π interactions. The distance between the centroids of the dinitroiodobenzene and dimethylamino pyridine rings is 3.657(2) and 3.718(2) Å with slippage of 1.55 and 1.78 Å respectively.

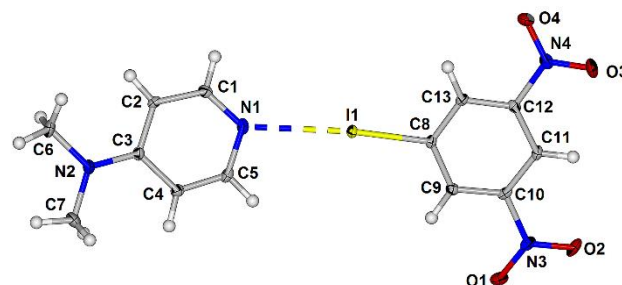


Fig. 1. Asymmetric unit of the halogen bonded cocrystal **A** formed between 3,5-dinitro-1-iodobenzene and 4-(*N,N*-dimethylamino)pyridine showing atom labelling. Displacement ellipsoids of non-H atoms are drawn at the 50% probability level and H atoms are shown as circles of arbitrary size. The halogen bond is shown as a dashed line.

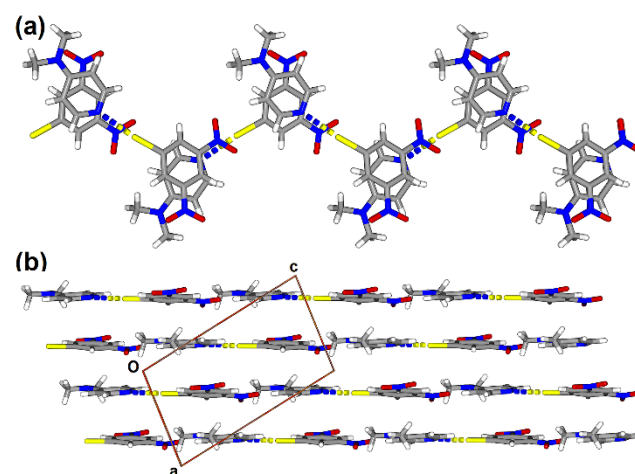


Fig. 2. Packing of the cocrystal **A** shown along the a axis (a) and b axis (b).

There are two non-conventional hydrogen bonds between nitro oxygen atoms and pyridyl hydrogen atoms with C-H...O distances of 2.48 and 2.57 Å and C-H...O angles of 150.0 and 165.5° respectively that support the formation of planar sheets of the cocrystals **A** shown in Figure 2.¹⁴

Molecular design, electrostatic potential calculations and synthesis.

The focus of our design was to separate, but maintain, the pyridine-iodobenzene halogen bonding interaction and the dinitrobenzene-dimethylaminoarene interaction that we reasoned was responsible for the charge transfer coloration. The first iteration of this design principle, described here, uses an alkyne to separate the halogen bond donor, tetrafluoroiodobenzene, from the π -acceptor, dinitrobenzene. Similarly the complementary halogen bond acceptor, pyridine, was connected to the π -donor *N,N*-dimethylaminobenzene with an ethynyl group. Our initial target molecules were thus

1-(3,5-dinitrophenylethynyl)-2,3,5,6-tetrafluoro-4-iodo benzene, **1**, and 4-[4-(N,N-dimethylamino)phenylethynyl] pyridine, **2**.

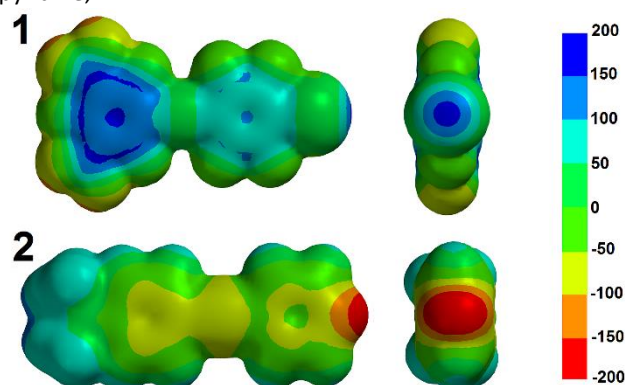
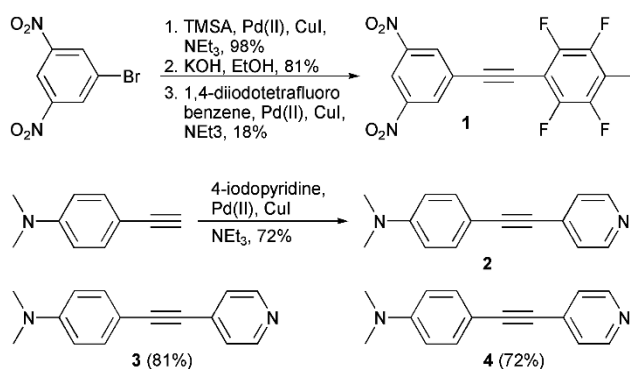


Fig. 3. Molecular electrostatic potential plots of **1** and **2** shown on the same scale in kJmol^{-1} .

Molecular electrostatic potential calculations were performed on **1** and **2** with the geometry constrained to the planar conformation before geometry minimization prior to calculating the electrostatic potential energy surface.¹⁵ For the halogen bond donor **1** the maximum value of the electrostatic potential associated with the σ -hole on the iodine atom is 180.6 kJmol^{-1} . Thus, based on the σ -hole on the iodine atom, **1** appears to be a better halogen bond donor than 1-iodo-3,5-dinitrobenzene and 1,4-diiodo-2,3,5,6-tetrafluorobenzene for which similar calculations yielded maximum values of the electrostatic potential associated with the σ -hole on the iodine atoms of 165.9 and 168.9 kJmol^{-1} respectively.¹⁶ The positive electrostatic potential spreads over both aromatic rings with a significant π -hole¹⁷ of 174.3 kJmol^{-1} in the center of the dinitro substituted benzene ring confirming the π -acceptor nature of the dinitrophenyl moiety (Fig. 3). It is noteworthy that the π -hole located at the centroid of 1-iodo-3,5-dinitrobenzene at 104.0 kJmol^{-1} is significantly weaker than that calculated for **1** reflecting the electron withdrawing effect of the 2,3,5,6-tetrafluoro-4-iodophenylethynyl moiety on the π -hole on the nitrosubstituted benzene ring. The minimum value of the electrostatic potential associated with the pyridyl nitrogen atom in **2** is $-201.0 \text{ kJmol}^{-1}$. This is lower than 4-(N,N-dimethylamino)pyridine, which has a minimum value of the electrostatic potential associated with the pyridyl nitrogen atom of $-220.5 \text{ kJmol}^{-1}$, presumably due to the more remote location of the electron donating N,N-dimethylamino group. Nevertheless we expected halogen bonding between the **1** and **2** to be similar to that between 1-iodo-3,5-dinitrobenzene and 4-(N,N-dimethylamino)pyridine. The negative electrostatic potential is spread across both aromatic rings with a minimum of -66.7 kJmol^{-1} in the dimethylaminophenyl ring and a minimum of -90.3 kJmol^{-1} located on the alkyne as shown in Figure 3. The minimum value of the electrostatic potential on the pyridine N atoms of the regioisomers 3-[4-(N,N-dimethylamino)phenylethynyl]pyridine, **3**, and 2-[4-(N,N-dimethylamino)phenylethynyl]pyridine, **4**, are -200.5 and $-215.8 \text{ kJmol}^{-1}$ respectively. It is noteworthy that the negative electrostatic potential in the dimethylamino substituted

benzene ring has a minimum of -75.3 and -81.9 kJmol^{-1} for **3** and **4** respectively. The syntheses of molecules **1-4** are outlined in Scheme 1. Thus, Sonogashira coupling of 1-bromo-3,5-dinitrobenzene with trimethylsilylacetylene (TMSA) followed by base deprotection gave 1-ethynyl-3,5-dinitrobenzene in good yield. Subsequent coupling with an excess of 1,4-diiodotetrafluorobenzene (Scheme 1) yielded **1** in low yield.



Scheme 1. Synthetic scheme for donor and acceptor molecules **1-4** used in this study.



Fig. 4. Photographs of individual colorless crystals of **1** (A); red cocrystals **B** (B); and fine crystalline precipitate of cocrystal **C** (C).

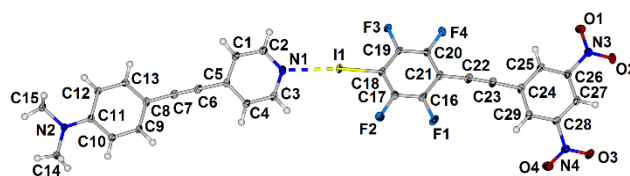


Fig. 5. Asymmetric unit of the halogen bonded cocrystal **B** formed between **1** and **2** with displacement ellipsoids of non-H atoms drawn at the 50% probability level and H atoms are shown as circles of arbitrary size. The halogen bond is shown as a dashed line.

Sonogashira coupling of 4-ethynyl-N,N-dimethylbenzylamine with 4-iodopyridine yielded **2** in good yield. The regioisomers of **2**, **3** and **4**, were similarly prepared by coupling with 3-iodopyridine and 2-bromopyridine respectively in good yield.

Cocrystallization, structural, spectral and computational analysis.

A uniform mass of red rod-shaped crystals, cocrystal **B**, was formed on slow evaporation of a dilute solution containing equimolar amounts of the colourless components **1** and **2** in dichloromethane (Fig. 4). The X-ray structure revealed that, as expected, the molecules **1** and **2** formed a 1:1 halogen bonded complex as shown in Figure 5. The halogen bond has a $\text{N}\cdots\text{I}$ distance of $2.798(2) \text{ \AA}$ with $\text{C-I}\cdots\text{N}$ angle of $172.4(1)^\circ$. The two methyl carbons are slightly below the plane of the dimethylamino phenyl ring, $0.035(5)$ and $0.142(5) \text{ \AA}$, and one

nitro group is slightly twisted with the oxygen atoms 0.184(5) Å above and 0.152(5) Å below the plane of the benzene ring. The two molecules **1** and **2** are slightly twisted with dihedral angles of 16.17(5) and 13.57(5) between the pyridyl and dimethylaminophenyl rings, and the tetrafluoroiodobenzene and the dinitrobenzene, respectively. The packing features asymmetric offset π -stacked molecules **1** and **2** with overlap between the dinitrophenyl and dimethylaminophenyl groups and the tetrafluoroiodophenyl and pyridyl groups as shown in Figure 6. The centroid to centroid distances between the dinitrophenyl ring and the dimethylaminophenyl rings is 3.695(2) and 3.747(2) Å with slippage of 1.33 and 1.65 Å and the centroid to centroid distance between the tetrafluoroiodophenyl ring and the pyridyl groups is 4.256(2) and 3.589(2) Å with slippage of 2.70 and 1.31 Å respectively (Table 4). Given the slightly twisted conformations of **1** and **2** it is not surprising that the crystal packing is complex. There are

two C-H...F interactions between adjacent molecules with H...F distances of 2.48 and 2.43 Å for H3...F3 and H10...F1 and C-H...F angles of 127.9 and 143.2 for C3-H3...F3 and C10-H10...F1 respectively.¹⁸ A bifurcated C-H...O contact to a nitro group has H12...O3 and H12...O4 distances of 2.79 and 2.80 Å respectively.

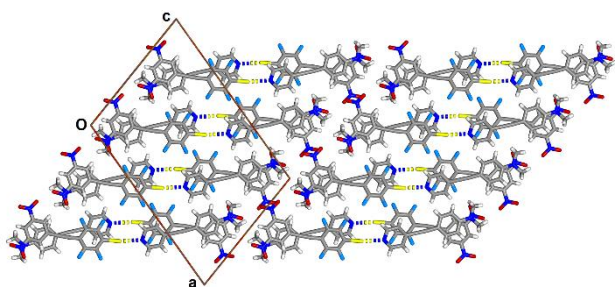


Fig. 6. Packing of cocrystal B viewed along the b axis.

Similar slow evaporation of separate equimolar solutions of each of the pyridyl regioisomers **3** and **4** with halogen bond donor **1** also resulted in red cocrystals, **C** and **D** respectively. Each cocrystal featured a 1:1 ratio of components with a strong halogen bond as shown in Fig. 7. In cocrystal **C** both individual components are essentially planar. One nitro group in **1** is coplanar with the benzene while the second nitro group is slightly twisted with oxygen atoms 0.199(9) Å above and oxygen 0.219(9) Å below the plane of the benzene. The dihedral angle between the planes defined by the tetrafluoroiodobenzene and the dinitrobenzene rings is 2.3(2). The dihedral angle between the planes defined by the dimethylaminophenyl and pyridyl rings 5.6(2). Surprising though the two molecules are not coplanar with a dihedral angle of 31.7(1) between the planes defined by the pyridyl and tetrafluoroiodobenzene rings. Thus the iodine atom is 0.631(9) Å out of the plane defined by the pyridine ring and the C-I...N bond angle is slightly bent at 169.9(2). The offset π -stacking, shown in Fig. 8, also features mixed stacks in which

the dinitrophenyl stacks between diaminophenyl groups similar to that observed in cocrystal **B**.

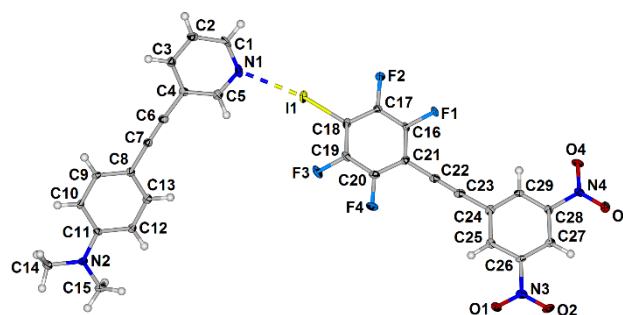


Fig. 7. Asymmetric unit of the halogen bonded cocrystal C formed between **1** and **3** with displacement ellipsoids of non-H atoms drawn at the 50% probability level and H atoms are shown as circles of arbitrary size. The halogen bond is shown as a dashed line.

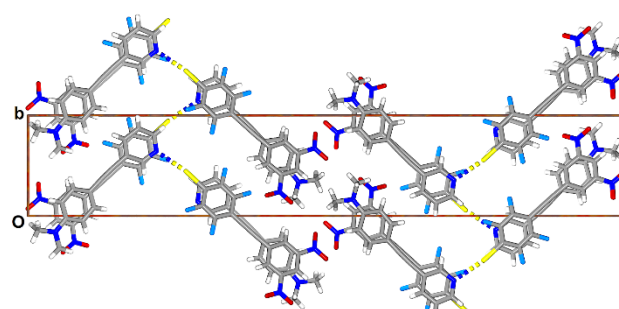


Fig. 8. Packing of the cocrystal C shown along the a axis.

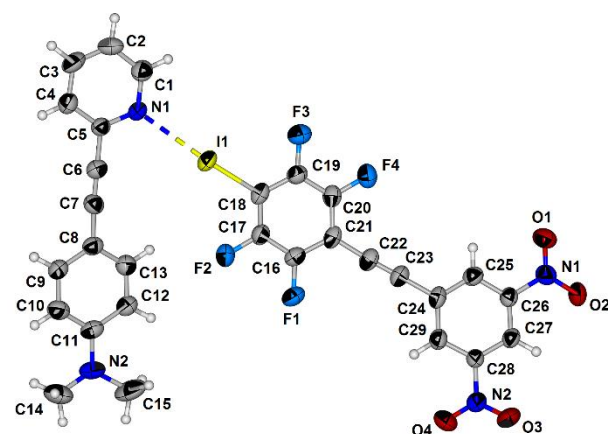


Fig. 9. Asymmetric unit of the halogen bonded cocrystal D formed between **1** and **4** with displacement ellipsoids of non-H atoms drawn at the 50% probability level and H atoms are shown as circles of arbitrary size. The halogen bond is shown as a dashed line.

In cocrystal **D** (Fig. 9) the components are almost planar. One nitro group in **1** is slightly twisted with the oxygen atoms 0.255(14) Å above and 0.300(14) Å below the plane of the benzene. The dihedral angle between the planes defined by the two benzene rings is 7.8(4) and the dihedral angle between the planes defined by the dimethylaminophenyl and pyridyl rings 5.2(3). The components **1** and **4** are slightly twisted from planarity with a dihedral angle of 10.1(3) between the planes

defined by the pyridyl and tetrafluoroiodobenzene rings and the iodine atom is only 0.27(1) Å out of the plane defined by the pyridine ring and the C-I...N bond angle is 175.8(3). The offset π -stacking also features mixed stacks in which the dinitrophenyl stacks between dimethylaminophenyl groups very similar to that observed in cocrystal **C** (Fig. 10). The weak non-conventional C-H...O and C-H...F hydrogen bonds in the structures of **C** and **D** are collected in Table 3.

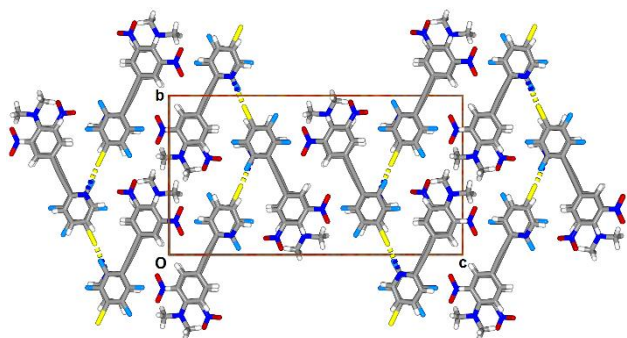


Fig. 10. Packing of the cocrystal **D** shown along the *a* axis

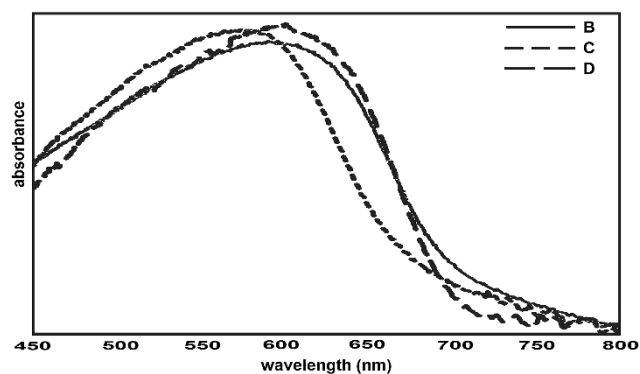
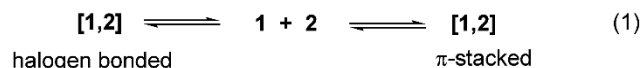


Fig. 11. Visible absorption spectra of the cocrystals **B**, **C** and **D** after subtraction of the normalized contribution of the individual components.

The visible absorption spectra of the red crystalline solids **B-D** were recorded along with the spectra of the essentially colorless individual components (**1-4**) and the contribution of the individual components subtracted to provide the visible absorbance unique to each individual cocrystal. These difference spectra in Figure 11 all feature a broad absorbance centered around 600 nm: specifically 593 nm for cocrystal **B**, 574 nm for cocrystal **C** and 602 nm for cocrystal **D**. These broad absorption bands are typical CT absorption bands observed with π -stacked arene donors and acceptors. In particular, *m*-dinitrobenzene formed a red CT cocrystal (3:1) with 1,3,5-tris(4-aminophenyl)benzene.¹⁹ We were unable to perform successful solution phase UV-visible studies of the complexation due to solubility issues at the concentrations needed.

Computational study of the relative halogen bond and charge transfer binding energies.

The crystal structures clearly show both halogen bonding and charge transfer complexation suggesting an interplay and competition between the two interactions (equation 1).



In order to address the interplay between halogen bonding and charge transfer complexation (equation 1) we calculated the relative binding energies of the halogen bonding interaction and the π -stacking interaction for three of the complexes. The coordinates taken from the X-ray structures were used as the starting point for the optimization of the structures. While there is a single unique halogen bonding interaction in each X-ray structure, each structure features two unique π - π interactions hence two independent initial geometries to minimize. For cocrystal **A**, the two optimized π - π structures starting from the two unique geometries optimized to mirror images of each other. For cocrystal **B**, the two optimized π - π structures are essentially identical. For cocrystal **C**, the two π -stacking structures did optimize to slightly different structures resulting in two slightly different values of the π - π binding energy. The binding energy for the π -stacked pair, 4-(*N,N*-dimethylamino)pyridine and 1-iodo-3,5-dinitrobenzene, is $-12.41 \text{ kcal mol}^{-1}$ compared to the halogen bond binding energy of $-7.75 \text{ kcal mol}^{-1}$. The halogen bond binding energy calculated for cocrystals **B** and **C** are similar, or slightly lower, than that of **A** (Table 4). In contrast, the π - π binding energy is significantly enhanced for larger π -systems at -18.78 to $-19.71 \text{ kcal mol}^{-1}$. Therefore π -stacking is favored, relative to halogen bonding, for the larger π -systems by more than 11 kcal mol^{-1} as compared to $4.66 \text{ kcal mol}^{-1}$ for the cocrystal **A**. Despite this, the molecular design clearly facilitates concomitant cooperative π -stacking and halogen bonding. Future computational studies of these and closely related matched complementary electron rich halogen bond acceptors and electron poor halogen bond donors will target the elucidation of the relative contributions of electrostatics, charge transfer, induction and dispersion to both the halogen bonding and the π -stacking interactions.¹⁷

Conclusions

The simple systems presented here confirm that cooperative halogen bonding and donor-acceptor π -stacking in cocrystallization is a viable concept. We plan to explore the incorporation of alternate donor and acceptor molecules as well as flexible spacers and functionalized spacers between the two interacting groups.

Experimental

Synthesis.

All solvents and reactants were used as purchased. All NMR spectra were recorded using CDCl₃ as solvent with Me₄Si as internal standard. All NMR coupling constants are given in Hz.

1-(3,5-Dinitro-phenylethynyl)-2,3,5,6-tetrafluoro-4-iodo-benzene, 1.

1-Ethynyl-3,5-dinitrobenzene (0.298 g, 1.50 mmol), bis(triphenylphosphine) palladium(II) chloride (60 mg, 0.09 mmol), copper iodide (20 mg, 0.10 mmol) and an excess of 1,4-diiodotetrafluorobenzene (1.25 g, 3.12 mmol) in a mixture of NEt₃ (5 mL) and THF (2 mL) were reacted at 55 °C for 3 h. The reaction mixture was cooled, diluted with CH₂Cl₂ and washed with brine. The organic layer was dried over Na₂SO₄, filtered and the solvent evaporated. The crude product was then purified by flash column chromatography on a silica gel. After flash column chromatography (hexane/EtOAc = 30:1), compound **1** was obtained as an off-white solid (0.206 g, 18%). Mp: 166.1-169.0 °C. ¹H NMR (400 MHz): δ 9.08 (1 H, t, *J* 2.3, Ph), 8.73 (2 H, d, *J* 2.3, Ph). ¹³C NMR (100 MHz): δ 148.6, 147.1 (ddt, *J* 260, 14, 4.5, 146.1 (ddm, *J* 259, 17.7), 131.5, 125.2, 119.2, 108 (t, *J* 23), 96.6 (t, *J*, 4), 79.6 (t, *J*, 4), 75.8 (t, *J* 28). ¹⁹F NMR (400 MHz): δ -133.54 (m, 2F), -118.77 (m, 2F). Found: C, 35.65; N, 5.35; H, 1.15. Calc. for C₁₄H₃F₄I₂N₂O₄: C, 36.1; N, 6.0; H, 0.65.

4-(4-Dimethylaminophenylethynyl) pyridine, 2.

4-Iodopyridine (0.42 g, 2.06 mmol), bis(triphenylphosphine) palladium(II) chloride (43 mg, 0.06 mmol), copper iodide (18 mg, 0.09 mmol), 4-ethynyl-N,N'-dimethylaniline (0.298, 2.06 mmol) in a mixture of NEt₃ (4 mL) and CH₂Cl₂ (4 mL) were reacted at room temperature for 24 h. The crude product was isolated as above to yield, after flash column chromatography with hexane/EtOAc = 4:1, compound **2** as an off-white solid (0.33 g, 1.49 mmol, 72%). Mp: 195.2-195.8 °C. ¹H NMR (400 MHz): δ 8.58 (2 H, d, *J*_{1,2} 5.9, Pyr), 7.42 (2 H, d, *J*_{1,2} 9.0, Ph), 7.33 (2 H, d, *J* 5.9, Pyr), 6.66 (2 H, d, *J* 9.0, Ph), 3.01 (6 H, s, NMe₂). ¹³C NMR (100 MHz): δ 150.9, 149.8, 133.4, 132.6, 125.4, 125.4, 111.9, 108.7, 96.2, 85.4, 40.3. Found: C, 80.03, N, 12.6; H, 6.35. Calc. for C₁₅H₁₀N₂: C, 81.05; N, 12.1; H, 6.35.

3-(4-Dimethylaminophenylethynyl) pyridine, 3.

3-Iodopyridine (0.74 g, 3.61 mmol), bis(triphenylphosphine) palladium(II) chloride (60 mg, 0.09 mmol), copper iodide (20 mg, 0.10 mmol), 4-ethynyl-N,N'-dimethylaniline (0.51 g, 3.51 mmol), NEt₃ (4 mL) and THF (6 mL) were reacted at room temperature for 24 h. The crude product was isolated as above to yield, after flash column chromatography with hexane/EtOAc=4:1, compound **3** was obtained as a slightly yellow solid (0.63 mg, 2.84 mmol, 81%). Mp: 133.8-134.1 °C. ¹H NMR (400 MHz): δ 8.73 (1H, d, *J* 1.6, Pyr), 8.48 (1 H, dd, *J* 4.7, *J* 1.6 Hz, 1 H), 7.75 (1, H, dt, *J* 7.8, *J* 2.0, Pyr), 7.42 (2 H, d, *J* 9.0 Hz, Ph), 7.24 (1 H, ddd, *J* 7.8, 4.7, 0.8, Pyr), 6.66 (2 H, d, *J* 9.0, Ph), 3.00 (s, 6 H, NMe₂). ¹³C NMR (100 MHz, CDCl₃): δ 148.8, 148.2 (m), 145.6 (m), 131.7, 125.4, 119.5, 103.5, 96.8, 79.9, 76.1 (m). Found: C,

80.1; N, 12.25; H, 6.3. Calc. for C₁₅H₁₀N₂: C, 81.05; N, 12.1; H, 6.35.

2-(4-Dimethylaminophenylethynyl) pyridine, 4.

2-Bromopyridine (0.26 g, 1.61 mmol), bis(triphenylphosphine) palladium(II) chloride (25 mg, 0.036 mmol), copper iodide (15 mg, 0.079 mmol), 4-ethynyl-N,N'-dimethylaniline (0.23 g, 1.57 mmol) in NEt₃ (3 mL) were reacted at 40 °C for 72 h. The crude product was isolated as above to yield, after flash column chromatography with hexane/EtOAc=4:1, compound **4** was obtained an off-white solid (0.25 mg, 1.13 mmol, 72 %). Mp: 100.1-101.2 °C. ¹H NMR (400 MHz): δ 8.58 (1 H, m, Pyr), 7.63 (1 H, td, *J* 7.6, *J* 2.0, Pyr), 7.48 (m, 3 H, 2H Ph and 1H Pyr), 7.16 (1 H, ddd, *J* 7.6, 5.9, 1.2, Pyr), 6.65 (2 H, d, *J* 9.0, Ph), 3.00 (6 H, s, NMe₂). ¹³C NMR (100 MHz): δ 150.7, 150.1, 144.5, 136.1, 133.5, 126.8, 122.1, 111.9, 108.9, 91.3, 87.3, 40.3. Found: C, 80.2; N, 12.0; H, 6.45. Calc. for C₁₅H₁₀N₂: C, 81.05; N, 12.1; H, 6.35.

Preparation of cocrystals. For cocrystal **B**, 0.020 mol of **1** and **2** were weighed into a small screw cap vial and 1 mL of dichloromethane added to form a clear yellowish solution. The vial was loosely capped and the solvent allowed to evaporate over the course of several days during which time a mass of red rod-shaped cocrystals formed. Cocrystals **C** and **D** were similarly prepared.

Electrostatic potential calculations. The geometry of molecules A-D were minimized with the two aromatic rings constrained in planar conformations and the electrostatic potential energy surface calculated using the Spartan'10 molecular modelling program with density functional theory (DFT) at the B3LYP/6-311+G** level.¹⁵ Minimal differences were obtained when the geometry corresponding to the crystal structures were used.

X-ray crystallography. Experiments were carried out at 100 K with Mo K α radiation using a Bruker APEX-II CCD diffractometer. Crystal data, data collection and structure refinement details are summarized in Table 1.²⁰ Absorption was corrected for by multi-scan methods. Refinement was with 0 restraints.²¹ All H atoms were located in difference maps. The methyl and phenyl hydrogens were treated as riding atoms in geometrically idealized positions with C—H = 0.95 (aromatic) and 0.98 Å (methyl) and Uiso(H) = kUeq(C), where k = 1.5 for the methyl hydrogens and 1.2 for the phenyl hydrogens. The program X-Seed was used as a graphical interface.²² The correct absolute configuration for the molecules of cocrystal **C** in the crystal selected for data collection was determined by the Flack x parameter of 0.015(9) by classical fit to all intensities and calculated using 2286

quotients $[(+)-(I-)]/[(+)+(I-)]$.²³ Cocrystal **D** formed as thin rod shaped crystals and after data collection from several crystals followed by refinement the program TwinRotMat was run using the PLATON interface.¹³ A TWIN law was determined and included in the refinement.

Computational study of interaction energies. For each of the crystalline complexes **A**, **B** and **C** the coordinates of the halogen bonded dimer and the two unique π - π charge transfer complexes were extracted and fully optimized in the gas-phase using the M062X²⁴ functional with the LANL2DZdp²⁷⁻²⁹ basis set on all atoms and the corresponding pseudopotential on iodine. All structures were verified to be local minima through vibrational frequency analysis. Counterpoise calculations were carried out according to the procedure of Boys and Bernardi.³⁰ All calculations were carried out using revision D.01 of the Gaussian 09³¹ suite of programs made available through XSEDE.³²

Solid state spectra. Electronic spectra of cocrystals and the individual components were recorded in solid state with the help of Cary 100 Bio spectrophotometer equipped with the solid-state accessory by Labsphere. The powdered compounds were spread over white Millipore filter and placed in the sample holder. The normalized spectra of each of the individual components were digitally subtracted from the normalized spectra of the cocrystals and the resultant difference spectrum.

Conflicts of interest

There are no conflicts to declare.

Acknowledgements

We thank the National Science Foundation for financial support of this research (CHE1606556), the Missouri State University Provost Incentive Fund that funded the purchase of the X-ray diffractometer, and the Missouri State University Graduate College for funding CIN. We thank Dr. Nikolay N. Gerasimchuk (MSU) for help measuring the solid-state visible spectra and Lauri Kivijärvi for help photographing the crystals. This work used the Extreme Science and Engineering Discovery Environment (XSEDE) resource Comet at the San Diego Supercomputing Center through allocation wis158. XSEDE is supported by the National Science Foundation grant number ACI-1548562. Additional computational resources were provided by NSF-MRI awards #CHE-1039925 and #CHE-0520704 through the Midwest Undergraduate Computational Chemistry Consortium--MU3C.

References

- (a) *Halogen Bonding: Fundamentals and Applications*, 2008, P. Metrangolo, G. Resnati (eds) (b) A. Priimagi, G. Cavallo, P. Metrangolo and G. Resnati, *Acc. Chem. Res.* 2013, **46**, 2686. (c) *Halogen Bonding I. Impact on Materials Chemistry and Life Sciences, Topics in Current Chemistry*, 2015, **358**. P. Metrangolo, G. Resnati (eds), 2015, Springer, Switzerland. (d) *Halogen Bonding I. Impact on Materials Chemistry and Life Sciences, Topics in Current Chemistry*, 2015, **359**. (e) P. S. Ho, *Future Med. Chem.*, 2017, 637-640. G. Cavallo, P. Metrangolo, R. Milani, T. Pilati, A. Priimagi, G. Resnati, G. Terraneo, *Chem. Rev.*, **2016**, **116**, 2478-2601.
- (a) K. Raatikainen, K. Rissanen *CrystEngComm*, 2009, **11**, 750. (b) N. R.; Goud, O. Bolton, E. C. Burgess, and A. J. Matzger *Cryst. Growth Des.* 2016, **16**, 1765-1771.
- (a) C. J. Kassel, D. C. Swenson, and F. C. Pigge *Cryst. Growth Des.* 2015, **15**, 4571-4580. (b) C. J. Massena, N. B. Wageling, D. I. A. Decato, E. M. Rodriguez, A. M. Rose, and O. B. Berryman *Angew. Chem. Int. Ed.* 2016, **55**, 12398-12402.
- (a) C. B. Aakeroy, C. L. Spartz, S. Dembowski, S. Dwyrea and J. Desper *IUCrJ*, 2015, **2**, 498-510. (b) M. D. Perera, J. Desper, A. S. Sinha and C. B. Aakeroy *CrystEngComm*, 2016, **18**, 8631-8636.
- K. P. Goetz, D. Vermeulen, M. E. Payne, C. Kloc, L. E. McNeil and O. D. Jurchescu, *J. Mater. Chem. C*, 2014, **2**, 3065-3076.
- (a) J. K. Kochi *Angew. Chem. Int. Ed. Engl.* 1988, **27**, 1227-1266. (b) S. V. Rosokha and J. K. Kochi *Acc. Chem. Res.* 2008, **41**, 641-653.
- S. Basu, A. Coskun, D. C. Friedman, M. A. Olson, D. Benitez, E. Tkatchouk, G. Barin, J. Yang, A. C. Fahrenbach, W. A. Goddard, III and J. F. Stoddart, *Chem. Eur. J.* 2011, **17**, 2107-2119.
- (a) T. Dahl, *Acta Chem. Scand.* 1973, **27**, 995-1003. (b) T. Dahl, *Acta Crystallogr., Sect. C: Cryst. Struct. Commun.* 1985, **41**, 931. (c) J. C. Collings, K. P. Roscoe, E. G. Robins, A. S. Batsanov, L. M. Stimson, J. A. K. Howard, S. J. Clark and T. B. Marder, *New J. Chem.*, 2002, **26**, 1740-1746.
- M. R. Bryce, S. R. Davies, M. B. Hursthouse, M. Motevalli *J. Chem. Soc., Perkin Trans. 2*, 1988, 1713-1716. (b) S. Keith McNeil, S. P. Kelley, C. Beg, H. Cook, R. D. Rogers, D. E. Nikles *ACS Appl. Mater. Interfaces* 2013, **5**, 7647-7653
- S. V. Rosokha and E. A. Loboda *J. Phys. Chem. A* 2015, **119**, 3833-3842.
- N. R. Goud and A. J. Matzger *Cryst. Growth Des.* 2017, **17**, 328-336.
- A. Bondi, *J. Phys. Chem.* 1964, **68**, 441-451.
- Calculated using Platon. A. L. Spek, *Acta Cryst. C*, 2015, **C71**, 9-18.
- (a) Desiraju, G. R. *Chem. Commun.*, 2005, 2995-3001. (b) Steiner, *S. Crystals*, 2015, **5**, 327-345.
- Spartan '10*, Version 1.0.1, Wavefunction, Inc. Irvine, CA, USA.
- C. B. Aakeroy, T. K. Wijethunga, J. Desper, and M. Đakovic *Cryst. Growth Des.*, 2016, **16**, 2662-2670.
- H. Wang, W. Wang and W. J. Jin, *Chem. Rev.* 2016, **116**, 5072-5104.
- V. R. Thalladi, H.-C. Weiss, D. Blaser, R. Boese, A. Nangia, G. R. Desiraju, *J. Am. Chem. Soc.* 1998, **120**, 8702.
- V. P. Vishnoi, M. G. Walawalkar and R. Murugavel *Cryst. Growth Des.* 2014, **14**, 5668-5673.
- Bruker (2014). SMART, SAINT and SADABS. Bruker AXS Inc., Madison, Wisconsin, USA.
- (a) G. M. Sheldrick, *Acta Cryst. Sect. A*, 2015, **A71**, 3-8. (b) G. M. Sheldrick, *Acta Cryst. Sect. C*, 2015, **C71**, 3-8.
- L. J. Barbour *J. Supramol. Chem.* 2001, **1**, 189-191.
- S. Parsons, H. D. Flack and T. Wagner, *Acta Cryst. Sect. B*, 2013, **B69**, 249-259.
- Y. Zhao and D. G. Truhlar. *Theor. Chem. Account.* **2008**, **120**, 215-241.

ARTICLE

Journal Name

- 25 T. H. Dunning, Jr. and P. J. Hay, *Gaussian Basis Sets for Molecular Calculations*. In *Modern Theoretical Chemistry*, H. F. Shaefer, III, (ed.) Plenum: New York, 1977, **3**, 1-28.
- 26 P. J. Hay, and W. R. Wadt, *J. Chem. Phys.* 1985, **82**, 270 – 283.
- 27 P. J. Hay, and W. R. Wadt, *J. Chem. Phys.* 1985, **82**, 284 – 298.
- 28 P. J. Hay, and W. R. Wadt, *J. Chem. Phys.* 1985, **82**, 299 – 310,
- 29 C. E. Check, T. O. Faust, J. M. Bailey, B. J. Wright, T. M. Gilbert, L. S. Sunderlin, *J. Phys. Chem. A*, 2001, **105**, 8111 – 8116.
- 30 S. F. Boys and F. Bernardi, *Mol. Phys.* 1970, **19**, 553 – 556.
- 31 M. J. Frisch, et al. Gaussian 09, Revision D.01; Gaussian, Inc: Wallingford, CT, 2009.
- 32 J. Towns, T. Cockerill, M. Dahan, I. Foster, K. Gaither, A. Grimshaw, V. Hazlewood, S. Lathrop, D. Lifka, G. D. Peterson, R. Roskies, J. R. Scott and N. Wilkins-Diehr, *Comput. Sci. Eng.* 2014, **16**, 62-74.

Table 1. Crystal data and structural refinement for cocrystals A – D.

	A	B	C	D
formula	C ₁₃ H ₁₃ IN ₄ O ₄	C ₂₉ H ₁₇ F ₄ IN ₄ O ₄	C ₂₉ H ₁₇ F ₄ IN ₄ O ₄	C ₂₉ H ₁₇ F ₄ IN ₄ O ₄
<i>M_r</i>	416.17	688.36	688.36	688.36
Crystal system	Monoclinic	Monoclinic	Orthorhombic	Monoclinic
space group	<i>P</i> 2 ₁ / <i>c</i>	<i>P</i> 2 ₁ / <i>c</i>	<i>P</i> 2 ₁ 2 ₁ 2 ₁	<i>P</i> 2 ₁ / <i>c</i>
Temp. (K)	100	100	100	100
<i>a</i> (Å)	7.1573 (3)	24.1533 (13)	7.2434 (5)	7.56541 (10)
<i>b</i> (Å)	16.8141 (7)	6.8223 (4)	7.9376 (5)	13.8231 (18)
<i>c</i> (Å)	12.5916 (5)	16.8260 (9)	47.215 (3)	26.027 (3)
β (°)	99.905 (1)	105.600 (1)	90	90.058 (2)
<i>V</i> (Å ³)	1492.73 (11)	2670.5 (3)	2714.6 (3)	2753.8 (6)
<i>Z</i>	4	4	4	4
μ (mm ⁻¹)	2.17	1.27	1.25	1.23
Crystal size (mm)	0.35 × 0.15 × 0.10	0.35 × 0.08 × 0.03	0.27 × 0.22 × 0.11	0.34 × 0.07 × 0.08
collected reflections	19222	31716	34837	35822
unique reflections	3298	6030	5977	6181
No. of parameters	201	381	381	382
<i>R</i> _{int}	1	0.044	0.053	0.031
<i>R</i> [<i>F</i> ² > 2σ(<i>F</i> ²)], <i>wR</i> (<i>F</i> ²),	0.018, 0.042	0.031, 0.073	0.037, 0.073	0.040, 0.113
Goodness of fit	1.09	1.03	1.16	1.06
CCDC	1820039	1820040	1820041	1820042

Table 2. Geometric parameters from crystal structures for A-D

Cocrystal	X...N dist. (Å, %) ^a	C-X...N angle (°)	DNP...DAP ^b centroid-to-centroid dist. (Å)	DNP...DAP perp. dist. ^c /slippage (Å)	TFIP...PYR ^d centroid-to-centroid dist. (Å)	TFIP...PYR perp. dist./slippage (Å)
A	2.894(2), 82.0	175.3(1)	3.657(1), 3.718(1) ^d	3.25/1.68	-	-
B	2.798(2), 79.3	172.4(1)	3.695(2), 3.747(2)	3.21/2.71	3.589(2), 4.260(2)	3.35/1.33
C	2.842(5), 80.5	169.9(2)	3.614(3), 3.746(3)	3.25/1.87	3.673(3), 3.675(3)	3.31/1.59
D	2.893(3), 82.0	175.7(2)	3.775(5), 3.886(5)	3.38/1.69	3.752(3), 3.907(3)	3.38/1.62

^a % of the sum of the van der Waals radii. ^bDNP = dinitrophenylring, DAP = N,N-dimethylaminophenyl/pyridine ring. ^c Shortest perpendicular distance to the centroid of one of the two rings. ^dTFIP = tetrafluoroiodophenylring, PYR = pyridine ring. ^d Distance between the centroids of the 1-iodo-3,5-dinitrobenzene and 4-N,N-dimethylaminopyridine rings.

Table 3. Hydrogen-bond geometry (Å, °) for A – D.

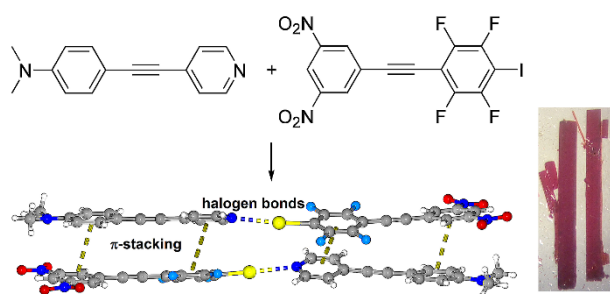
Cocrystal	D—H...A	D-H	H...A	D...A	D-H...A
A	C2—H2...O1i	0.95	2.57	3.501 (2)	165.5
	C5—H5...O3ii	0.95	2.48	3.333 (2)	150.0
B	C3—H3...F3i	0.95	2.48	3.153 (3)	127.9
	C10—H10...F1ii	0.95	2.43	3.246 (3)	143.2
	C12—H12...O3iii	0.95	2.79	3.468 (3)	128.9
C	C12—H12...O4iii	0.95	2.80	3.747 (3)	172.4
	C2—H2...F3i	0.95	2.41	3.342 (6)	169.0
	C12—H12...F1ii	0.95	2.51	3.286 (6)	139.0
	C14—H14A...O4iii	0.98	2.59	3.226 (7)	122.8
	C14—H14B...O3iv	0.98	2.61	3.564 (7)	164.8
D	C14—H14C...O3v	0.98	2.59	3.496 (7)	153.5
	C13—H13...F2	0.95	2.57	3.337 (6)	137.5
	C4—H4...O2i	0.95	2.63	3.519 (6)	156.1
	C1—H1...O4ii	0.95	2.65	3.478 (6)	146.5

Table 4. Binding energies calculated from separated halogen bonded and π -stacked charge transfer dimers^a

Cocrystal	XB binding energy	π - π binding energy
A	-7.75	-12.41
B	-7.72	-19.30
C	-7.43	-19.71
		-18.78 ^b

^a Counterpoise corrected energies in kcalmol⁻¹. ^b Value calculated for second optimized π -stacked dimer (text).

Table of Contents Entry



Matched electron rich halogen bond acceptors and donor have been synthesized and the halogen bonded charge transfer cocrystals characterized.